Available online at www.sciencedirect.com
ScienceDirect
Geochimica et Cosmochimica Acta 72 (2008) 1742–1757
Geochimica et Cosmochimica Acta
www.elsevier.com/locate/gca

# Copper isotope fractionation during its interaction with soil and aquatic microorganisms and metal oxy(hydr)oxides: Possible structural control

O.S. Pokrovsky [a,*], J. Viers [a], E.E. Emnova [b], E.I. Kompantseva [c], R. Freydier [a]

[a] *Laboratoire de Mécanismes et Transfert en Géologie (LMTG), Université de Toulouse, CNRS, IRD, OMP, 14 Avenue Edouard Belin, 31400 Toulouse, France*
[b] *Institute of Genetics and Plant Physiology, Moldavian Academy of Science, Kishinev, Moldavia*
[c] *Institute of Microbiology, Russian Academy of Science, Moscow, Russia*

Received 4 June 2007; accepted in revised form 23 January 2008; available online 31 January 2008

**Abstract**

This work is aimed at quantifying the main environmental factors controlling isotope fractionation of Cu during its adsorption from aqueous solutions onto common organic (bacteria, algae) and inorganic (oxy(hydr)oxide) surfaces. Adsorption of Cu on aerobic rhizospheric (*Pseudomonas aureofaciens* CNMN PsB-03) and phototrophic aquatic (*Rhodobacter* sp. f-7bl, *Gloeocapsa* sp. f-6gl) bacteria, uptake of Cu by marine (*Skeletonema costatum*) and freshwater (*Navicula minima*, *Achnanthidium minutissimum* and *Melosira varians*) diatoms, and Cu adsorption onto goethite (FeOOH) and gibbsite (AlOOH) were studied using a batch reaction as a function of pH, copper concentration in solution and time of exposure. Stable isotopes of copper in selected filtrates were measured using Neptune multicollector ICP-MS. Irreversible incorporation of Cu in cultured diatom cells at pH 7.5–8.0 did not produce any isotopic shift between the cell and solution ($\Delta^{65/63}$Cu(solid-solution)) within ±0.2‰. Accordingly, no systematic variation was observed during Cu adsorption on anoxygenic phototrophic bacteria (*Rhodobacter sp.*), cyanobacteria (*Gloeocapsa sp.*) or soil aerobic exopolysaccharide (EPS)-producing bacteria (*P. aureofaciens*) in circumneutral pH (4–6.5) and various exposure times (3 min to 48 h): $\Delta^{65}$Cu(solid-solution) = 0.0 ± 0.4‰. In contrast, when Cu was adsorbed at pH 1.8–3.5 on the cell surface of soil the bacterium *P. aureofaciens*having abundant or poor EPS depending on medium composition, yielded a significant enrichment of the cell surface in the light isotope ($\Delta^{65}$Cu (solid-solution) = −1.2 ± 0.5‰). Inorganic reactions of Cu adsorption at pH 4–6 produced the opposite isotopic offset: enrichment of the oxy(hydr)oxide surface in the heavy isotope with $\Delta^{65}$Cu(solid-solution) equals 1.0 ± 0.25‰ and 0.78 ± 0.2‰ for gibbsite and goethite, respectively. The last result corroborates the recent works of Mathur et al. [Mathur R., Ruiz J., Titley S., Liermann L., Buss H. and Brantley S. (2005) Cu isotopic fractionation in the supergene environment with and without bacteria. *Geochim. Cosmochim. Acta* **69**, 5233–5246] and Balistrieri et al. [Balistrieri L. S., Borrok D. M., Wanty R. B. and Ridley W. I. (2008) Fractionation of Cu and Zn isotopes during adsorption onto amorhous Fe(III) oxyhydroxide: experimental mixing of acid rock drainage and ambient river water. *Geochim. Cosmochim. Acta* **72**, 311–328] who reported heavy Cu isotope enrichment onto amorphous ferric oxyhydroxide and on metal hydroxide precipitates on the external membranes of Fe-oxidizing bacteria, respectively.

Although measured isotopic fractionation does not correlate with the relative thermodynamic stability of surface complexes, it can be related to their structures as found with available EXAFS data. Indeed, strong, bidentate, inner-sphere complexes presented by tetrahedrally coordinated Cu on metal oxide surfaces are likely to result in enrichment of the heavy isotope on the surface compared to aqueous solution. The outer-sphere, monodentate complex, which is likely to form between $Cu^{2+}$ and surface phosphoryl groups of bacteria in acidic solutions, has a higher number of neighbors and longer bond distances compared to inner-sphere bidentate complexes with carboxyl groups formed on bacterial and diatom surfaces

* Corresponding author.
*E-mail address:* oleg@lmtg.obs-mip.fr (O.S. Pokrovsky).

0016-7037/$ - see front matter 
doi:10.1016/j.gca.2008.01.018

in circumneutral solutions. As a result, in acidic solution, light isotopes become more enriched on bacterial surfaces (as opposed to the surrounding aqueous medium) than they do in neutral solution.

Overall, the results of the present study demonstrate important isotopic fractionation of copper in both organic and inorganic systems and provide a firm basis for using Cu isotopes for tracing metal transport in earth-surface aquatic systems. It follows that both adsorption on oxides in a wide range of pH values and adsorption on bacteria in acidic solutions are capable of producing a significant (up to 2.5–3‰ (±0.1–0.15‰)) isotopic offset. At the same time, Cu interaction with common soil and aquatic bacteria, as well as marine and freshwater diatoms, at $4 < pH < 8$ yields an isotopic shift of only ±0.2–0.3‰, which is not related to Cu concentration in solution, surface loading, the duration of the experiment, or the type of aquatic microorganisms.


## 1. INTRODUCTION

Numerous experimental works have demonstrated that stable isotope systems of iron, zinc, and copper may potentially provide valuable proxies for a wide range of geochemical processes involving abiotic and bacterially mediated fractionation phenomena in low-temperature environments (Anbar et al., 2000; Brantley et al., 2001; Beard et al., 2003; Albarède, 2004; Mathur et al., 2005; Anbar and Rouxe, 2007; Borrok et al., 2008). However, prior to the interpretation of isotope measurements in natural settings, rigorous calibration of isotopic fractionation in the laboratory is necessary.

Compared to other heavy metals, copper is particularly interesting as it combines versatile chemical properties and molecular structures with multiple oxidation states (+1 and +2) both in solution and in solid. It is extremely toxic for all aquatic photosynthetic microorganisms (i.e., Soldo and Behra, 2000). This toxicity is usually explained through a mechanism of blocking and reducing the thiol sites on proteins. Although a significant amount of work has been devoted to Cu(II) ion binding to algal (e.g., Xue et al., 1988; Xue and Sigg, 1990; Gonzalez-Davila, 1995; Knauer et al., 1997, 1998; Gonzalez-Davila et al., 2000) and bacterial (He and Tebo, 1998; Daughney et al., 1998; Fowle and Fein, 1999; Kunito et al., 2001;Claessens and Van Cappellen, 2007) surfaces and metal oxides (Weesner and Bleam, 1997; Peacock and Sherman, 2004), as well as Cu complexation with organic ligands in freshwater (Wu and Tanoue, 2001; Hoffmann et al., 2007), the isotopic fractionation associated with these reactions remains largely unknown.

Copper is able to engage in a variety of complexes, notably hydrates and halides, with very different coordinations such as square planar, square pyramidal, trigonal pipyramidal and tetragonal complexes (c.f., Alcacio et al., 2001; Pasquarello et al., 2001) including polynuclear components. This ability is the source of rather strong isotopic variation, with maximum variability of Cu isotope compositions observed in hydrothermal ores (Zhu et al., 2000; Larson et al., 2003; Rouxel et al., 2004; Markl et al., 2006).

Only a few experiments have documented Cu isotopic fractionation under controlled laboratory conditions. Reduction of aqueous Cu(II) into insoluble Cu(I) brings about an enrichment of up to 4‰ in the solid phase in the light isotope (Zhu et al., 2002; Rouxel, 2002). For Cu(II) precipitation from solution in the form of sulfide, Ehrlich et al. (2004) reported $\Delta^{65}$Cu (CuS-solution) ~3‰ which is much higher than the value of 0.2–0.4‰ for Cu(II) precipitation in the form of malachite (Maréchal and Sheppard, 2002). Cu fractionation on anion exchange resin AG-MP1 was observed in 7 M HCl: $^{63}$Cu is more effectively retained on the column, producing about 0.4‰ isotopic offset (Maréchal et al., 1999; Maréchal and Albarède, 2002). Zhu et al. (2002) demonstrated that Cu isotope fractionation induced by the uptake of Cu proteins in yeast is similar in magnitude to that produced during Cu uptake into azurine, and the proteins are approximately 1–2‰ isotopically lighter relative to their source. The reduction of Cu(II) into Cu(I) accompanied through Cu interaction with proteins can explain this isotopic shift. Abiotic oxidation of Cu sulfide led to 1.3–2.7‰ heavy isotope enrichment in solutions, as compared to the starting material, whereas the presence of Fe-oxidizing bacteria (*Thiobacillus ferrooxidans*) in Cu sulfide oxidation reaction produced isotopically light fluids due to the uptake of $^{65}$Cu on metal oxides formed on the external membranes of these cells (Mathur et al., 2005). Consistent with this finding, fractionation of Cu isotopes during adsorption onto amorhous ferric oxyhydroxide yields $\Delta_{\text{solid-solution}} = 0.73 \pm 0.08$‰ (Balistrieri et al., 2008). Release of isotopically heavy adsorbed Cu from regenerated particulate organic material has been invoked to explain the variation of $\delta^{65}$Cu (0.5‰) in the NE Pacific water column, although the authors acknowledged the major analytical challenges involved in determining Cu-isotopes in seawater (Bermin et al., 2006). For other heavy elements, it has been widely argued that molecular mechanisms operating at solid/solution interfaces are likely to be responsible for isotopic fractionation (Johnson et al., 2004). For example, isotopic fractionation of Zn (Cacaly et al., 2004; Rousset et al., 2004; Pokrovsky et al., 2005b), Ge (Galy et al., 2002) and Mo (Barling and Anbar, 2004) has been reported during adsorption onto solid oxy(hydr)oxides.

This study presents a first step toward quantitative experimental calibration of Cu(II) isotope fractionation between aqueous solution and organic and inorganic sorbents that are ubiquitous in the earth-surface environment. Using a series of rigorously designed equilibrium and kinetic experiments, we addressed the following questions: (i) what are the sign and the magnitude of Cu isotopic fractionation depending on solution pH, the nature of the solid and the duration of interaction, and (ii) is it possible to relate the isotopic fractionation produced by Cu interaction with microorganisms and mineral oxides to the stability and

structure of surface complexes that are formed? We hope that answering these questions will provide a firm basis for quantitative use of copper isotopes as proxies for tracing biogeochemical processes in surficial aquatic environments.

## 2. MATERIAL AND METHODS

### 2.1. Culture of microorganisms

Anoxygenic photosynthetic purple bacteria, *Rhodobacter* sp. f-7bl, and mesophilic cyanobacteria, *Gloeocapsa* sp. f-6gl, were obtained from the collection of the Laboratory of Ecology and Geochemical Activity of the Microorganisms (Winogradsky Institute of Microbiology, Moscow, Russia). Purple bacteria were cultured anaerobically on mineral Pfenning medium with an addition of 0.1 g/L of yeast extract and 2 g/L of malate and pH 7.4. *Gloeocapsa* sp. cyanobacteria were cultured on D medium (Pfennig and Trüper, 1989) at pH 8.0–8.2. The typical conditions of culture were the following: a light intensity of 2–3 thousands lux, temperature 28–30 °C, and stationary growth phase achieved after 1–2 weeks. The growth phase was assessed by measuring optical density or cell biomass as a function of time.

The bacterial strain of soil aerobic gram-negative bacteria *Pseudomonas aureofaciens* CNMN PsB-03 was obtained from the laboratory of the Plant Mineral Nutrition and Hydric Regime (Institute of Plant Genetics and Physiology, Moldovan Academy of Sciences, Chishinau, Moldova). The specific strain was isolated from soybean root-adhering (rhizosferic) soil (Emnova et al., 2005); they were selected due to their capacity for producing large amounts of gel-forming exopolysacharide (EPS) on a sucrose-peptone (SP) medium (Behrens and Ringpfeil, 1963). This strain synthesizes and excretes an extracellular fluorescent yellow–green pigment-siderophore with high affinity for $Fe^{3+}$ ions (pioverdin—with hynoline chromophore and peptide chain as the main molecular components). On sugar-poor medium (0.4% succinic acid, AS, Meyer and Abdallah, 1978), this strain provides only poor synthesis of EPS. The isolated strain is also able to produce a large amount of intracellular yellow–orange pigments (2-hydroxyphenazine-1-carbonic acid and 2-hydroxyphenazine) on both SP and AS media. The *Pseudomonas* sp. was maintained at 4 °C in AS media (as broth and agar slant cultures). For biomass accumulation the strain was cultured in SP and AS media for 48 h at 28 °C. Cells were harvested at the beginning of the stationary phase. Two samples of *P. aureofaciens* PsB-03 biomass were used in the present study. The first sample consisted of cells growing in nutritive medium with sucrose as a single carbon source, which yields an abundant EPS synthesis, and the second was composed of cells growing in nutritive medium with succinic acid as a single carbon source, which produces very poor EPS. In addition to differences in the amount of EPS produced on SP and AS media, the qualitative monosaccharide composition of produced exopolymers is also different (Emnova et al., 2007). In the EPS produced on SP media, fructose constituted 76.1% of total sugars, and the second dominant monosaccharide was glucose (11.4%). The monosaccharides from EPS produced on AS media are composed of 49.9% glucose, 22.3% fructose, and 14% mannose. Small amounts (<10% of total sugars) of rhamnose, ribose, xylose, and galactose were present in both EPS samples. These data indicate that the polysaccharide levan (polyfructan) is the most probable EPS of *P. aureofaciens* in SP medium, and glucan and some other heteropolymers are present in AS medium. Note that according to Sutherland (1982), the differences between exopolysaccharides and polysaccharides on bacterial cell walls are rather approximate and subject to strong variations depending on cell surface physical modification and aging.

Monospecific diatom cultures of marine planctonic *Skeletonema costatum* (SC), freshwater periphytic *Achnanthidium minutissimum*(AMIN), *Navicula minima* (NMIN) and *Melosira varians* (MVAR) were produced as described previously (Gélabert et al., 2004, 2006, 2007). Diatoms were cultured to a concentration of $\sim 10^7$ cell/L at 20 °C in sterile Dauta (freshwater) or f/2 (seawater) media (Gold et al., 2003) at pH 7.5–7.8 and $[Cu]_{tot} \sim 0.2$ μM. Continuous aeration of the culture was provided to prevent pH from increasing due to photosynthetic activity. Typical incubation time was 1–2 weeks. Diatoms were harvested from the late exponential—stationary growth phase and kept at 4 °C for 3–5 days until use. Bacteria were cultured to the beginning of the stationary growth phase and used immediately for adsorption experiments.

The biomass of live bacteria and diatom cell suspensions were quantified by measuring humid (centrifuged 25 min at 4500*g*) and dry (liophylized) weight. Before the adsorption experiment, cells were rinsed three times in appropriate 0.01 or 0.1 M $NaNO_3$ solution using centrifugation at 4500*g* ($\sim$ 500 mL of solution for 1 g of wet biomass) to remove, as much as possible, the adsorbed metals and cell exudates from the surface. The conversion factors humid/dry(liophylised) weight for studied microorganisms were the following: *A. minutissimum*, 17.6; *N. minima*, 10.0; *S. costatum*, 6.2; *Rhodobacter* sp., 11.7; *Gloeocapsa* sp., 8.2; EPS-rich *P. aurefaciens*, 3.6; EPS-poor *P. aurefaciens*, 5.0.

### 2.2. Metal oxy(hydr)oxides

Synthetic goethite FeOOH (Pokrovsky et al., 2006, specific surface area (SSA) of 23.2 $m^2/g$) and gibbsite $Al(OH)_3$ (Prolabo®, SSA = 2.87 $m^2/g$) were used in the present study. The specific surface area of solids was measured using a Micromeritics ASAP 2010 apparatus according to the B.E.T. technique with multiple points (i.e., typically 10) of nitrogen adsorption. Uncertainty about the BET SSA measurements was less that 10% as estimated from a linear regression analysis procedure. The crystallinity of minerals was verified using X-ray diffraction. Before the experiments, all solids were reacted 30 min in 0.01 M ultrapure $HNO_3$, thoroughly rinsed in deionized Milli-Q® water and conditioned in $N_2$-saturated, 0.01 M $NaNO_3$ for at least one week prior to the experiments. Trace element analysis of the studied solids using ICP-MS (Elan 6000, Perkin Elmer) did not detect any impurities within $\leqslant$0.1 wt.%, and Cu content was below 10 ppm. All reagents were of analytical grade or better. Suprapure $NaNO_3$ (Merck®) was used

as a background electrolyte. Suprapure Cu(II) sulfate or nitrate were used as a source of Cu in adsorption experiments.

### 2.3. Copper adsorption experiments

Copper adsorption experiments were designed to provide a quantitative characterization of Cu binding on microorganism and oxide surfaces in a wide range of pH and Cu(II) concentrations in solution in order to test whether there is a correlation between the adsorption constant and the magnitude of isotope fractionation. Two types of experiments were performed: (i) adsorption at constant initial copper concentration in solution as a function of pH (pH-dependent adsorption edge) and (ii) adsorption at constant pH as a function of copper concentration in solution (adsorption isotherm). Furthermore, the influence of time of exposure in kinetic experiments was also investigated. All experiments were performed in solutions that were undersaturated with respect to any solid copper oxide, hydroxide or carbonate phases as verified by using the MINTEQA2 computer code and corresponding database (Allison et al., 1991; Martell et al., 1997).

Adsorption experiments were conducted at $25 \pm 0.2$ °C in a continuously stirred suspension of 0.01 or 0.1 M $NaNO_3$ solution using 8 mL sterile polypropylene vials. The biomass concentrations were held constant at 4 or 10 g humid/L and copper concentration in solution ($[Cu^{2+}]_{aq}$) spanned from 0.2 to 50 μM. The pH was adjusted to the desired value using either NaOH or $HNO_3$. HEPES buffer, which is known not to form complexes with divalent metals in aqueous solutions (Mirimanoff and Wilkinson, 2000), was added to a concentration of 0.003 M in order to keep pH constant during adsorption isotherm measurements. For all experiments, sterile de-ionized water (MilliQ, 18 mΩ) purged of $CO_2$ by $N_2$ bubbling was used. At the end of the experiment, the suspension was centrifuged and the resulting supernatant was filtered through a 0.22 μM Nylon filter, acidified with ultrapure nitric acid and stored in the refrigerator until analysis. The concentration of copper adsorbed to solid in each vessel was calculated by subtracting the concentration of copper in the supernatant from the original amount of metal added in the suspension. Blank experiments of Cu release from the biomass as a function of pH and Cu adsorption on the reactor wall in suspension-free solution at various pH levels were run for each experiment and did not demonstrate, within the range of analytical uncertainty, Cu contamination from the cells or Cu adsorption on reactor walls in the full range of pH.

Exposure time varied from 0.5 min to 43 h in order to assess the kinetic factor in the Cu adsorption process. For most experiments, exposure time was fixed to 2–3 h. Optical microscopic inspection of bacterial cells before and after adsorption experiments showed no visible change in the cell structure and shape. The cells remained intact and non-deformed, and no cell fragments could be detected.

The reversibility of Cu adsorption equilibria was first tested following the method developed by Fowle and Fein (2000). A homogeneous parent suspension solution of bacteria + Cu + electrolyte was adjusted to pH ~7 at which 100% Cu was adsorbed onto microbial cells. After 3 h of adsorption contact time, aliquots of this parent suspension solution were taken and adjusted to sequentially lower pH values (2–6.9). The reaction vessels were equilibrated at new pH values for 3 h and then sampled for Cu. The concentration of desorbed copper in the supernatant allowed for calculation of the amount of irreversibly assimilated metal. This amount never exceeded 5–10%, suggesting an equilibrium adsorption process with a negligible amount of copper penetrating inside the cell. The acidification method was considered inappropriate for the microbial sorbents due to the possibility of cell damage at low pH (Borrok et al., 2004). Thus, the second reversibility test, used earlier for algae and bacteria (Slaveykova and Wilkinson, 2002; Smiejan et al., 2003), consisted of treating the cell suspension with 0.01 M EDTA solution at neutral pH for 2–3 min, separating the cells and the supernatant by centrifugation, and filtering and measuring dissolved (<0.2 μm) copper concentration in the filtrate. The first method was tested for Fe and Al oxides while the second method was employed for checking the reversibility of copper adsorption on soil bacteria *P. aureofaciens*. In all cases, very good recovery (>95%) of adsorbed copper was achieved, suggesting a truly reversible adsorption process.

### 2.4. Analytical methods

All filtered solutions were analyzed for Cu ($[Cu]_{aq}$) using flame atomic absorption (AAS, Perkin Elmer 5100 PC spectrophotometer) with an uncertainty of ±1% and a detection limit of 0.1 μM. For Cu concentration lower than 0.5 μM, analyses were performed by ICP-MS on a Perkin Elmer SCIEX, Elan 6000 with a detection limit of 1 nM and a precision of ±10% and 5% for 1–50 and 50–500 nM, respectively. Cu concentration in the solid phase was measured by AAS after full acid digestion of this phase (concentrated $HNO_3$ for oxy(hydr)oxides and $HNO_3 + H_2O_2$ for cells) was performed in the clean room. Values of pH were measured using a Mettler Toledo® combined electrode, which has an accuracy of ±0.002 units. Dissolved Organic Carbon (DOC) was analyzed using a Carbon Total Analyzer (Shimadzu TOC-5000) with an uncertainty of 3% and a detection limit of 0.1 ppm.

### 2.5. Cu stable isotope measurements

For experiments of Cu uptake by diatoms, both the initial solution and growing biomass were analyzed, while for the adsorption experiments on bacteria and oxides, only filtered solution was processed. Diatom cells harvested by centrifugation at 2500*g* were dried at 80 °C and ground using agate mortar and pestle. The first portion of ground material was always discarded. One hundred milligrams of ground powder was submitted to hydrogen peroxide digestion ($H_2O_2$) followed by acid digestion ($HNO_3 + HF$) in a clean bench room following a procedure used for vegetation samples (i.e., Viers et al., 2007). Blank tests were performed to estimate the level of Cu contamination induced by the digestion procedure and were found to be less

than 0.2% (0.02–0.1 ppm) of the less concentrated sample. The international geostandard SRM 1515 (Apple Leaves, from NIST, USA) was used to check the validity and the reproducibility of both the acid digestion and ICP-MS analyses. The relative difference between our values and the certified data was close to 5%. This allowed us to check for an efficient recovery of the copper after the acid digestion. Even if we consider 95% of Cu recovery after acid digestion, a mass balance calculation reveals that this should not affect, within the range of external reproducibility, the global isotopic signature of the sample.

In isotopic fractionation experiments, a full recovery of filtered solution during the preparation procedure is crucial (i.e., Barling and Anbar, 2004; Anbar, 2004). Filtration of supernatant in adsorption type experiments did not affected the fractionation coefficients because filtration of the initial Cu stock solution did not change $\delta^{65}$Cu within the uncertainty ($\pm 0.05‰$) as verified by (i) Multi Collector ICP MS measurements on this filtered sample subjected to ion-column purification procedure, and (ii) a $100 \pm 1\%$ recovery of $[Cu]_{aq}$ in filtered standard solutions at pH 5–6 as measured by AAS.

Cu isotopic composition was measured at Toulouse (LMTG) on the Neptune MC-ICP-MS (ThermoFinnigan). Cu has two stable isotopes of mass 63 and 65, which have average abundances of 69.17% and 30.83%, respectively. Cu was isolated from the bulk sample using the purification procedure of Maréchal et al. (1999) on the AGMP-1 anion exchange resin (Bio-Rad, USA). Poly-Prep chromatography columns ($0.8 \times 4$ cm) (Bio-Rad, USA) were used for the elemental separation. After the resin was cleaned (1.6 mL) with MilliQ deionized water (18.2 Ω) and 0.5 N $HNO_3$, the conditioning of the resin (6 mL) and the loading of the sample (300 ng of Cu in 1 mL) were performed with 7 N HCl. The hydrogen peroxide was added into the acid solution at a 0.001% concentration to avoid the presence of Cu in a different redox state. The matrix was eluted with 10 mL of 7 N HCl and Cu was collected in the next fraction (20 mL of 7 N HCl). Because isotopic fractionation may occur during the elemental separation on the ion-exchange resin (Maréchal and Albarède, 2002), we analyzed only the samples for which the separation procedure produced a 100% yield, taking into account the analytical uncertainties.

The Neptune introduction system used in this study consists of a tandem quartz glass spray chamber (cyclone + standard Scott double pass) coupled with a low flow PFA nebulizer (50–70 µl/min.). Ar gas flows of 15, 1.2, and 0.6 L/min were used for coolant, nebulizer and auxiliary, respectively. For ICP operation, an RF generator with power of 1300 W was used. The cup configuration allowed simultaneous collection of the two Cu isotopes and the four Zn masses (64, 66, 67, 68) for mass bias correction, and in addition to (Zn/Ni), mass 62 to check for eventual Ni interferences (Maréchal, 1998). After a minimum of four hours of instrument warm up and calibration, analytical sequences were run automatically using a Cetac ASX-100 autosampler. Between each sample and standard, the machine was rinsed with 0.05 N $HNO_3$ from two different vials for 1 min each. Blank measurements consist of 1 block of 10 cycles (8s) and sample and standard measurements consist of 2 blocks of 20 cycles of 8s each. For a single measurement (40 cycles), internal precision was found to be between 5 and 10 ppm ($2\sigma$) for both Cu and Zn isotopic ratios.

The $^{62}$Ni signal was simultaneously measured to evaluate the isobaric interference of $^{64}$Ni on the $^{64}$Zn signal; no significant interference was found. Instrumental mass fractionation was corrected following the method described by Maréchal et al. (1999). A Zn standard (JMC 3-0749L) was added to the purified Cu fractions and a Cu (NIST 976) + Zn (JMC 3-0749L) standard mixture was run as a bracketing standard. The concentration of Cu and Zn in the sample or standard is kept at the same level (300 µg/l). Indeed, it has been reported that a difference of concentration between the internal standard (Zn) and the measured element (Cu) may induce problems for mass bias correction (Archer and Vance, 2004). The ratio of Cu and Zn fractionation factors (i.e., $f_{Cu}/f_{Zn}$) was found to be constant over a single analytical session (i.e., one day measurement) for the Neptune instrument. As observed by Maréchal et al. (1999) and Pichat et al. (2003) this $f_{Cu}/f_{Zn}$ ratio does not remain constant from one day to another. The slope of the fractionation line derived from the standard mixture raw data in a $\ln(^{66}Zn/^{64}Zn)$ versus $\ln(^{65}Cu/^{63}Cu)$ plot was used to correct the data on the Cu sample + Zn standard mixtures. Note that these fractionation lines were drawn with the different Zn isotopic ratios ($^{66}$Zn/$^{64}$Zn, $^{67}$Zn/$^{64}$Zn, $^{68}$Zn/$^{64}$Zn, and $^{68}$Zn/$^{66}$Zn). The Cu isotopic results in this study are given in the recommended delta notation for the $^{65}$Cu/$^{63}$Cu ratio (Albarède, 2004):

$$\delta^{65}Cu = [((^{65}Cu/^{63}Cu)_s/(^{65}Cu/^{63}Cu)_{NIST976}) - 1] * 1000\ (in‰) \quad (1)$$

where s signifies sample and NIST 976 the Cu isotopic standard solution. Note that the Zn JMC 3-0749L solution used during analysis is not a referenced material but an elemental standard solution used by several laboratories and provided by the Lyon group. The uncertainty given in the Table 2 for the $\delta^{65}$Cu in each sample is the $2\sigma$ (sigma standard deviation of the average of 10 $\delta^{65}$CuNIST measurements made over the course of the day) calculated using the average of three different methods of correction (bracketing, external normalization using different Zn/Cu ratio and exponential law, see Viers et al., 2007). For long-term irreversible uptake on growing diatom cells and soil bacteria, and reversible sorption on bacteria, the $2\sigma$ varies between 0.03‰ and 0.08‰ (see Table 2). For Zn sorption on metal oxides and on viable soil bacteria, the $2\sigma$ is higher, probably reflecting less efficient purification during column separation procedure. The external reproducibility obtained on samples analyzed in Lyon (ENS, P54) and in Toulouse (LMTG, Neptune) is around 0.1‰.

For batch adsorption experiments performed in a closed system, the isotopic signature of the solid phase ($\delta^{65}Cu_{solid}$) was calculated from the mass balance equation using the isotopic ratio in the aqueous phase ($\delta^{65}Cu_{aq}$), the amount of metal adsorbed ($A$, %), and the isotopic composition of initial solution ($\delta^{65}Cu_{initial}$):

$$\delta^{65}Cu_{solid} = \{100 \cdot \delta^{65}Cu_{initial} - (100 - A) \cdot \delta^{65}Cu_{aq}\}/A \quad (2)$$

In this work, we define the isotopic offset between Cu in solution and Cu adsorbed on bacteria and oxides or incorporated in diatom cells as

$$\Delta^{65}Cu(\text{solid-solution}) = \delta^{65}Cu_{solid} - \delta^{65}Cu_{aq} \quad (3)$$

Since for most experiments only the solid phase was analyzed, we evaluated the associated errors via measuring total Cu retained in the solid phase. After full acid digestion of the solid, we found a recovery of Cu between 90% and 95%. Assuming the "worst" scenario, 90% recovery, we calculated the error produced in the final ($\Delta^{65}$Cu(solid-solution) calculation for each data point from Eqs. (2) and (3). In most cases, the errors are smaller or comparable with internal errors of isotopic ratio measurements. Only for short-term reversible adsorption on soil bacteria (series 3), the error bars increased from 0.05‰ to 0.1–0.15‰ (Table 2).

## 3. EXPERIMENTAL RESULTS

### 3.1. Adsorption on oxy(hydr)oxides

The percentage of adsorbed copper on goethite and gibbsite is plotted as a function of pH in Figs. 1 and 2, respectively. In accord with previous studies (Stumm, 1992), adsorption of Cu onto oxy(hydr)oxides is negligible at pH below 3–5 and increases to 100% adsorbed at pH above 6–8. The reversibility tests of Cu adsorption on gibbsite and goethite fully revealed equilibrium processes within ±10% uncertainty that is comparable to the experimental reproducibility.

A simple thermodynamic model for the oxy(hydr)oxide-solution interface was used in this study to rationalize the adsorption results. This model postulates the existence of

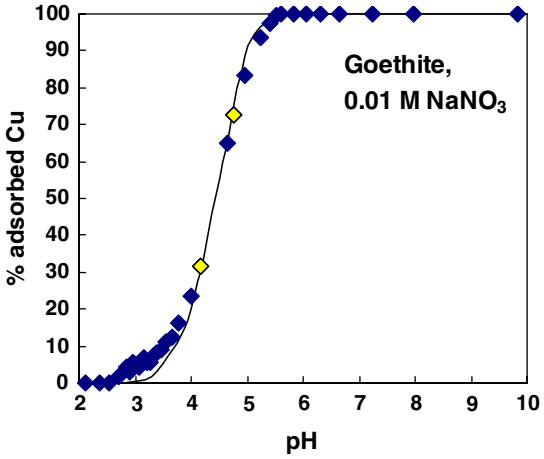


Fig. 1. Adsorption of copper (II) on goethite as a function of pH. Experimental conditions: exposure time 24 h in the dark, 0.01 M NaNO3, $[Cu]_o = 8.2$ μM, 76.6 $m^2$/L of goethite surface. The symbols represent results of adsorption experiments, but the curves were generated from the surface complexation model (SCM) using $\log K_6 = 2.2 \pm 0.2$. The open symbols represent the experiments used for isotopic analysis.

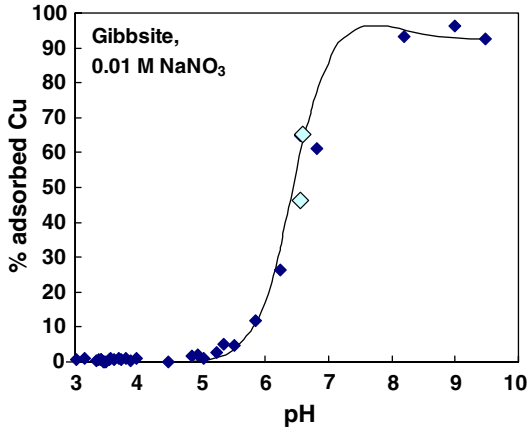


Fig. 2. Adsorption of copper (II) on gibbsite as a function of pH. Experimental conditions: exposure time 24 h in the dark, 0.01 M $NaNO_3$, $[Cu]_o = 8.2$ μM, 31.3 $m^2$/L of gibbsite surface. The symbols represent results of adsorption experiments, but the curves were generated from the surface complexation model (SCM) using $\log K_6 = 0.5 \pm 0.1$. Open symbols represent the experiments used for isotopic analysis.

one primary hydration site, >MeOH° (Me = Fe, Al). This site undergoes protonation or deprotonation forming $MeOH_2^+$ and $>MeO^-$ surface species, respectively. Thus, copper adsorption onto oxy(hydr)oxide surfaces was modeled using a 2-p$K$ constant capacitance model (CCM). For this modeling, all Surface Complexation Model (SCM) parameters (p$K$, site densities and $C$) were taken from work of Sverjensky and Sahai (1996). Surface site density was set to 16 μmol/$m^2$, electric double layer capacitance to 1 F/$m^2$ and intrinsic surface stability constants for reactions:

$$> MeOH^\circ + H^+ => MeOH_2^+, \quad \log K_4 \quad (4)$$

$$> MeOH^\circ - H^+ => MeO^-, \quad \log K_5 \quad (5)$$

were borrowed from Sverjensky and Sahai (1996). $\log K_4$ equals 6.9 (goethite) or 7.0 (gibbsite); $\log K_5$ equals −10.7 (goethite) or −10.9 (gibbsite). The CCM is the simplest SCM, and while it has some disadvantages as compared to the more commonly used triple layer model, it requires a minimal amount of adjustable parameters (Lützenkirchen, 1999). The only adjustable parameter in this study is the stability constant for Cu adsorption in the form of a mononuclear complex:

$$> MeOH^\circ + Cu^{2+} => MeO\text{-}Cu^+ + H^+, \quad \log K_6 \quad (6)$$

This parameter was varied to reproduce the experimental data (solid lines in Figs. 1 and 2). The modeling was performed using MINTEQA2/PRODEFA2 computer codes (Allison et al., 1991).The fit was done by trial and error and the minimal sum of difference between the fitted and measured values was considered to be a criterion of the goodness of fit. A close description of the experimental pH-dependent adsorption edges was achieved with $\log K_6$ equal to $2.2 \pm 0.2$ (goethite) and $0.5 \pm 0.1$ (gibbsite). The surface adsorption constant is about two orders of magnitude higher for goethite compared to gibbsite. Using the same set of surface protonation constants and SCM param-

eters, Pokrovsky et al. (2005b) reported $K_6$ for $Zn^{2+}$ adsorption onto goethite and gibbsite that was 1–2 orders of magnitude lower than that for $Cu^{2+}$. This difference probably reflects the different affinity of Cu and Zn to functional groups of oxide surfaces, as is the case with other sorbents (cf. Fein et al., 2001).

### 3.2. Adsorption on bacteria

Measurement of copper adsorption kinetics on bacteria diatom cells indicates that a majority of Cu is sorbed after 0.3–1 min and that the rate of sorption is quite slow and can last up to 100 min (Fig. 3), which is in agreement with previous works on metal adsorption onto bacteria (Fein et al., 1997; Ngwenya et al., 2003), green algae (Gonzales-Davila et al., 1995; Xue et al., 1988), and diatoms (Gonzalez-Davila et al., 2000; Gélabert et al., 2006, 2007).

In order to determine whether Cu adsorbed to cell surface functional groups or to organic exudates, we monitored dissolved organic carbon. We found that the concentration of dissolved organic carbon in the set of adsorption experiments at pH from 1.5 to 11.5 did not systematically change by more than 30–50%. Thus, only weak degradation of the cell wall in the pH range used for the adsorption experiments was observed. Low dissolved organic carbon concentration monitored during adsorption experiments (i.e., 3–10 mg/L) and relatively high Cu and cell biomass concentration (1.5–50 μM and 4–10 g/L, respectively) imply that bacterial surface functional groups, and not organic exudates, are primarily responsible for Cu binding in the systems studied.

Results of copper adsorption experiments on *P. aureofaciens* as a function of pH are depicted in Fig. 4. For both cell samples (after abundant and poor EPS production), the general trend is a strong increase in adsorption at pH $\geqslant$ 1 and complete removal of Cu at pH > 3–3.5. Bacterial cells grown with intensive EPS production exhibit higher adsorption capacities of Cu from solution at 3 < pH < 5 (Fig. 4). This is further illustrated in Fig. 5, where adsorption isotherms at pH 5.85 and 0.5 < [Cu] < 50 μM are plotted. Adsorption onto EPS-rich cells is stronger in the full range of Cu(II) concentration studied.

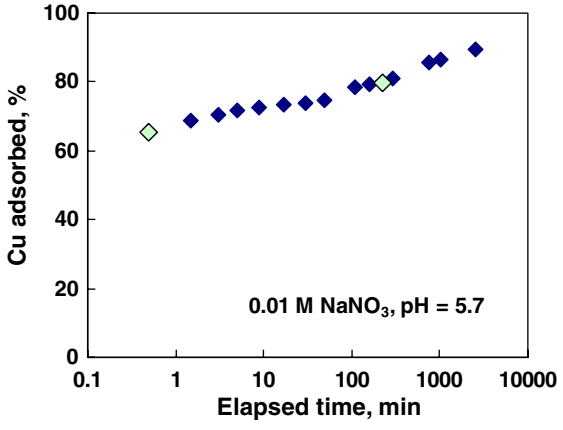


Fig. 3. Kinetics of copper(II) adsorption on *Rhodobacter sp.* Experimental conditions: 0.01 M $NaNO_3$, 4 g humid/L of bacteria, $[Cu^{2+}]_o = 49$ μM, pH 5.70. Open symbols represent the experiments used for isotopic analysis.

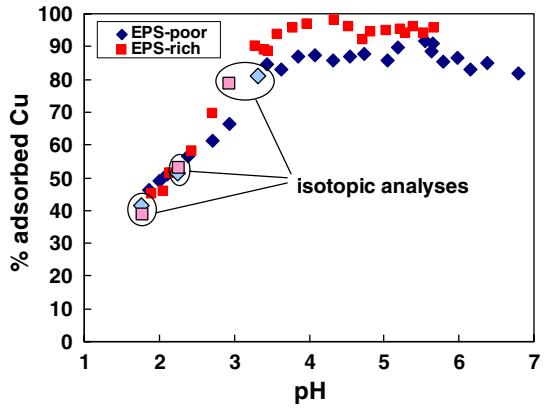


Fig. 4. Adsorption of copper (II) on soil EPS-producing bacteria *P. aureofaciens* CNMN PsB-03 as a function of pH. Experimental conditions: exposure time 2 h in the dark, 0.1 M $NaNO_3$, $[Cu]_o = 52$ μM, 10 g humid/ L. Diamonds, cells after poor EPS synthesis; squares, cells after abundant EPS production.

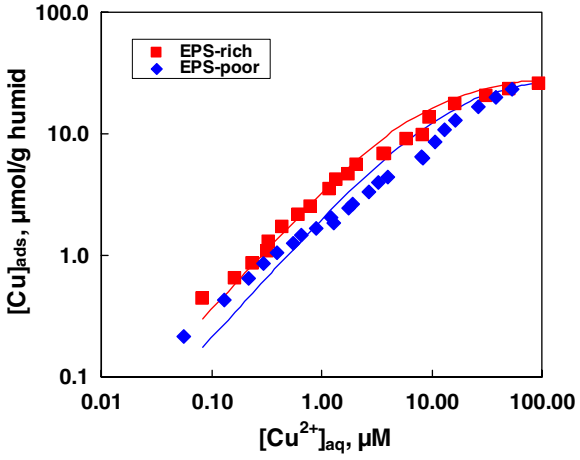


Fig. 5. Adsorption of copper (II) on soil bacteria *P. aureofaciens* as a function of copper concentration in solution. Experimental conditions: exposure time 2 h in the dark, 0.1 M $NaNO_3$, 10 g humid biomass $L^{-1}$. The symbols represent results of adsorption experiments, and the curves represent Langmurian adsorption isotherm generated using parameters listed in Table 1. Diamonds, cells after poor EPS synthesis, pH 5.85 ± 0.15; squares, cells after abundant EPS production, pH 6.10 ± 0.05.

Adsorption of copper onto *Rhodobacter sp.* is depicted in Fig. 6 (adsorption isotherm at pH 5.4) and Fig. 7 (pH-dependent adsorption edge). Although the adsorption capacities of anoxygenic phototrophs are similar to soil *Pseudomonas* (compare Figs. 5 and 6), the maximum adsorption on the latter occurs at ~2 pH units lower (Figs. 4 and 7).

Adsorption of copper on cyanobacteria (*Gloeocapsa sp.*) is illustrated in Fig. 8 in the form of a Langmuirian adsorption isotherm. It can be seen from a comparison of Figs. 5, 6 and 8 that the wet biomass-normalized binding capacities

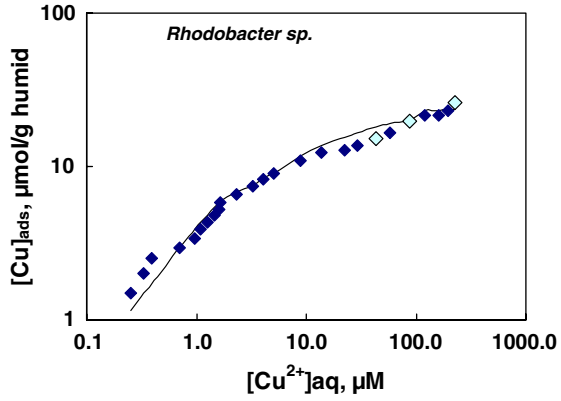


Fig. 6. Adsorption of copper (II) on anoxygenic phototrophic bacteria *Rhodobacter* sp. Experimental conditions: exposure time 3 h in the dark, 0.01 M $NaNO_3$, 4 g humid/L of biomass, pH $5.4 \pm 0.2$. The symbols represent results of adsorption experiments, and the curves represent Langmurian adsorption isotherm generated using parameters listed in Table 1. Open symbols represent the experiments used for isotopic analysis.

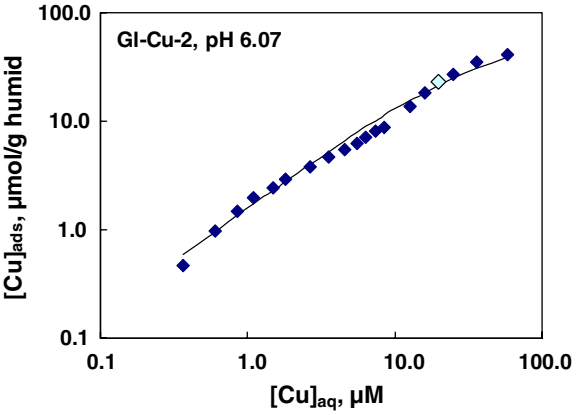


Fig. 8. Adsorption of copper (II) on cyanobacteria *Gloeocapsa*sp. Experimental conditions: exposure time 3 h in the dark, 0.01 M $NaNO_3$, 4 g humid/L of biomass, pH $6.07 \pm 0.07$. The symbols represent results of adsorption experiments, and the curve represents Langmurian adsorption isotherm generated using parameters listed in Table 1. The open symbol represents the experiment used for isotopic analysis.

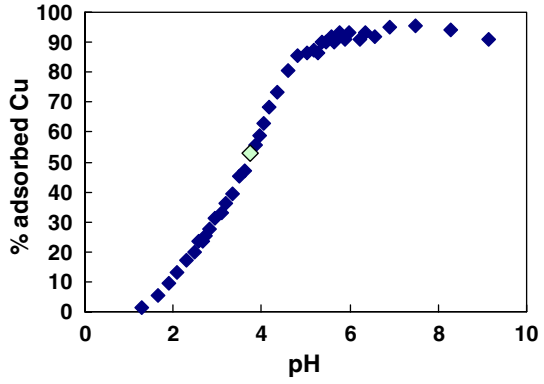


Fig. 7. Adsorption of copper (II) on anoxygenic phototrophic bacteria *Rhodobacter* sp. f-7bl as a function of pH. Experimental conditions: exposure time 3 h in the dark, 0.01 M $NaNO_3$, $[Cu]_o = 20$ µM, 4 g humid/L of biomass. The open symbol represents the experiment used for isotopic analysis.

of bacterial cells at pH 5.4–6 are similar among all three bacteria species studied in this work.

Since the acid–base surface titrations necessary to define the chemical nature and acidity of surface functional groups on all three bacteria are not available, rigorous surface complexation modeling of metal adsorption onto bacterial surfaces (i.e., Fein et al., 1997) cannot be performed. The adsorption reaction on solid surfaces, including the interaction of one ion on one surface site, can be written as:

$$> S^- + Cu^{2+} => S\text{-}Cu^+ \quad (7)$$

where $>S^-$ is the surface site, and $>S\text{-}Cu^+$ is the adsorbed complex. The conventional stability constant of this reaction ($K_L$) is defined as:

$$K_L = \{> S\text{-}Cu^+\}/(\{> S^-\} \cdot [Cu^{2+}]) \quad (8)$$

where {} is the surface concentration and [] stands for aqueous metal concentration. The concentration of adsorbed metal ($\Gamma_{ads}$) is represented by the Langmuir equation:

$$\Gamma_{ads} = \{> S\text{-}Cu^+\} = (K_L \cdot \Gamma_{max} \cdot [Cu^{2+}])/(1 + K_L \cdot [Cu^{2+}]) \quad (9)$$

where $\Gamma_{max}$ is the maximal adsorbed concentration corresponding to occupation of all surface sites available at a given pH. The parameters of Eq. 9 for all of the studied species are listed in Table 1 and the model fit to the data is presented as solid line in Figs. 5, 6 and 8. Parameters of the Langmuir equation are similar for soil bacteria and anoxygenic phototrophs, whereas the cyanobacteria *Gloeocapsa* sp. exhibits 2–3 times higher adsorption capacitance, but a half an order of magnitude lower adsorption constant compared to other bacteria. It is possible that both the pH of the experimental solution, which is the highest for cyanobacteria, and the specific surface structure of *Gloeocapsa* sp., such as presence of thick polysaccharide sheath or capsule, is responsible for this difference. Copper binding capacities of all bacteria studied in this work (20–60 µmol/g humid or ~200–600 µmol/g dry weight) are consistent with available measurements of divalent metals on other bacteria and algae (e.g., Fein et al., 1997; Klimmek

Table 1
Parameters of Langmuir (9) equation for studied bacteria. Reported uncertainties are $2\sigma$ values calculated from minimum 10 experimental data points

| Species | pH | $K_L(\times 10^6)$ | $\Gamma_{max}$, µMol/g humid |
|---|---|---|---|
| *P. aureofaciens* (EPS-rich) | $5.85 \pm 0.15$ | $0.12 \pm 0.01$ | $30 \pm 5$ |
| *P. aureofaciens* (EPS-poor) | $6.10 \pm 0.05$ | $0.07 \pm 0.005$ | $30 \pm 5$ |
| *Rhodobacter* sp. f-7bl | $5.4 \pm 0.2$ | $0.18 \pm 0.02$ | $22 \pm 2$ |
| *Gloeocapsa*sp.*f-6gl* | $6.07 \pm 0.07$ | $0.025 \pm 0.005$ | $65 \pm 5$ |

et al., 2001; Davis et al., 2003; Gélabert et al., 2005) as well as carboxylate site concentrations on gram-negative bacteria (Ngwenya et al., 2003; Guiné et al., 2006; Dittrich and Sibler, 2005).

### 3.3. Stable isotope fractionation

The results of stable isotope measurements are reported in Table 2 and illustrated in Fig. 9. Analyses of digested cells from marine and freshwater diatom culturing experiments in the presence of Cu (samples SC, AMIN, NMIN and MVAR) revealed enrichment of marine planktonic cells *S. costatum* by heavy isotope ($\Delta^{65}$Cu(solid-solution) = 0.23 ± 0.05‰), comparable with that for Zn (0.27–0.08‰, Gélabert et al., 2006). In contrast, freshwater species *A. minutissimum*, *N. minima* and *M. varians* did not demonstrate any significant fractionation between aqueous culture media and the cells ($\Delta^{65}$Cu(solid-solution) = 0.0–0.1‰).

In neutral solution, the sorption of Cu on growing rhizospheric *P. aureofaciens* (sample 4-2 G) did not produce an isotopic fractionation, within the uncertainty range of 0.2‰. However, short-term reversible sorption on viable bacteria in acidic solutions at 1.8 ⩽ pH ⩽ 3.3 (samples 2-1 to 2-8; 3-1 to 3-9) yielded clear enrichment of cells by light isotope with $\Delta^{65}$Cu(solid-solution) ranging from −0.9‰ to −1.4‰ for EPS-poor and EPS-rich production, respectively. For the latter, no systematic effect of pH in the range of 1.8–2.9 could be detected.

Short-term reversible sorption on anoxygenic phototrophic *Rhodobacter* sp. (samples Cu–K-1 and Cu–K-11) produced the same isotopic shift after 0.5 and 224 min of exposure ($\Delta^{65}$Cu(solid-solution ~0.3‰). The sorption at pH 3.8–5.4 at various surface loadings (2.6–26 μmol/g humid, samples F7-Cu-1-14 to F7-Cu-2-25) did not yield any systematic isotopic offset between the surface and solution with $\Delta^{65}$Cu(solid-solution) ranging from −0.3‰ to 0.5‰. Finally, sorption of Cu onto *Gloeocapsa* sp. cyanobacteria at neutral pH (sample Gl-Cu-2) did not produce any measurable fractionation. Therefore, both "passive" reversible adsorption on and "active" uptake (assimilation) of Cu by aquatic and soil microorganisms at 4 ⩽ pH ⩽ 8 do not yield systematic isotopic offset between aqueous solution and cell biomass with $\Delta^{65}$Cu(solid-solution) maximal range from −0.3‰ to +0.5‰ and typical values ~0 ± 0.2‰. Only sorption in acidic solutions (1.8 ⩽ pH ⩽ 3.3) produced fractionation: $-0.6 < \Delta^{65}\text{Cu(solid-solution)} < -1.8$.

Iron and aluminum oxy(hydr)oxides at 4.2 ⩽ pH ⩽ 6.1 exhibit an enrichment of the surface in heavy isotope by 0.6–1.3‰, producing statistically similar fractionation for gibbsite and goethite: $\Delta^{65}$Cu(solid-solution) = 1.0 ±

Table 2
Results of stable isotopic fractionation. In series (1), (2) and (3), the initial Cu salt $\delta^{65}Cu_{initial} = 0.056 \pm 0.023$‰

| Sample | Exposure | pH | $[Cu]_{aq}$, μM after exp. | % Cu adsorbed | $\delta^{65}Cu_{aq}$ (‰) | $\delta^{65}Cu_{solid}$ (‰) | $\Delta^{65/63}Cu_{solid/solution}$ (‰) |
|---|---|---|---|---|---|---|---|
| (1) Long-term irreversible uptake in growing diatom cells (culture medium, 20 °C, under light) | | | | | | | |
| SC | 2 weeks | 7.8 ± 0.2 | 0.2 ± 0.05 | N.D. | 0.018 ± 0.047 | 0.24 ± 0.05 | 0.23 ± 0.05 |
| AMIN | 3 weeks | 7.7 ± 0.2 | 0.2 ± 0.05 | N.D. | 0.24 ± 0.05 | 0.19 ± 0.05 | −0.05 ± 0.05 |
| NMIN | 3 weeks | 7.6 ± 0.2 | 0.2 ± 0.05 | N.D. | 0.24 ± 0.05 | 0.23 ± 0.05 | −0.01 ± 0.05 |
| MVAR | 3 weeks | 7.7 ± 0.2 | 0.2 ± 0.05 | N.D. | 0.24 ± 0.05 | 0.12 ± 0.05 | −0.12 ± 0.05 |
| (2) Reversible sorption on growing *Pseudomonas aureofaciens* cells from culture medium (35 °C, darkness) | | | | | | | |
| 4-2 G *P. aureofaciens* | 48 h | 5.89 | 18 | 50.9 | 0.144 ± 0.224 | −0.03* | −0.17 ± 0.22 |
| (3)Short-term reversible sorption on viable rhizospheric bacteria *P. aureofaciens* (25 °C, darkness), 0.1 M $NaNO_3$ | | | | | | | |
| 2-1, EPS | 2 h | 1.78 | 32 | 39 | 0.49 ± 0.04 | −0.63* | −1.12 ± 0.15 |
| 2-5, EPS | 2 h | 2.27 | 25 | 53 | 1.01 ± 0.04 | −0.79* | −1.80 ± 0.15 |
| 2-8, EPS | 2 h | 2.93 | 11 | 79 | 1.04 ± 0.03 | −0.21* | −1.26 ± 0.03 |
| 3-1, EPS-poor | 2 h | 1.76 | 31 | 42 | 0.31 ± 0.04 | −0.31* | −0.62 ± 0.15 |
| 3-5, EPS-poor | 2 h | 2.25 | 25 | 52 | 0.56 ± 0.04 | −0.42* | −0.99 ± 0.10 |
| 3-9, EPS-poor | 2 h | 3.32 | 9.9 | 81 | 1.01 ± 0.03 | −0.17* | −1.18 ± 0.04 |
| (4)Short-term reversible sorption on viable *Rhodobacter* sp. (25 °C, darkness), 0.01 M $NaNO_3$ | | | | | | | |
| Cu-K-1# | 0.5 min | 5.70 | 16.8 | 66 | −0.17 ± 0.02 | 0.12* | 0.29 ± 0.05 |
| Cu-K-11# | 224 min | 5.70 | 9.9 | 80 | −0.19 ± 0.08 | 0.07* | 0.26 ± 0.08 |
| F7-Cu-1-14# | 3 h | 3.76 | 9.4 | 53 | 0.03 ± 0.04 | 0.01* | −0.02 ± 0.05 |
| F7-Cu-2-19# | 3 h | 5.38 | 43 | 58 | −0.02 ± 0.03 | 0.05* | 0.07 ± 0.03 |
| F7-Cu-2-21# | 3 h | 5.14 | 87.5 | 48 | 0.18 ± 0.02 | −0.15* | −0.32 ± 0.02 |
| F7-Cu-2-25# | 3 h | 5.08 | 225 | 32 | −0.13 ± 0.02 | 0.36* | 0.49 ± 0.10 |
| (5) Short-term reversible sorption on viable *Gloeocapsa* sp. (25 °C, darkness), 0.01 M $NaNO_3$ | | | | | | | |
| Gl-Cu-2# | 3 h | 6.07 | 20 | 82 | 0.07 ± 0.03 | 0.01* | −0.05 ± 0.03 |
| (6) Sorption on metal oxy(hydr)oxides, 0.01 M $NaNO_3$ | | | | | | | |
| AlOOH-23 | 24 h | 6.09 | 2.8 | 65 | −0.77 ± 0.32 | 0.49* | 1.26 ± 0.32 |
| AlOOH-34 | 24 h | 6.06 | 4.4 | 46 | −0.31 ± 0.12 | 0.48* | 0.79 ± 0.12 |
| FeOOH G-24 | 24 h | 4.16 | 5.6 | 32 | −0.26 ± 0.16 | 0.73* | 0.98 ± 0.16 |
| FeOOH G-26 | 24 h | 4.76 | 2.2 | 73 | −0.37 ± 0.06 | 0.21* | 0.58 ± 0.07 |

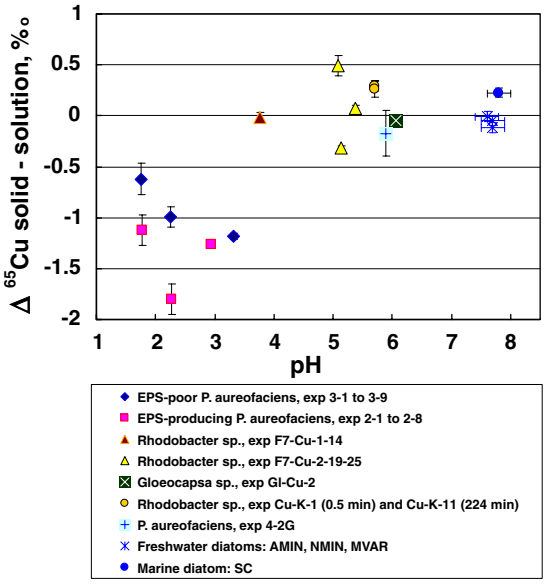


Fig. 9. Isotopic offset between solution and cell surfaces (Eq. (3)) for copper adsorption on and uptake by bacteria and diatoms as a function of solution pH. Experimental conditions are listed in Table 2. These error bars stem from analytical errors of isotope measurements as described in Section 2.5. Rigorously propagated error due to uncertainty on [Cu] analysis in solid and solution is included in each error bar. For some data points, the error bars are within the size of the symbols (see Table 2).

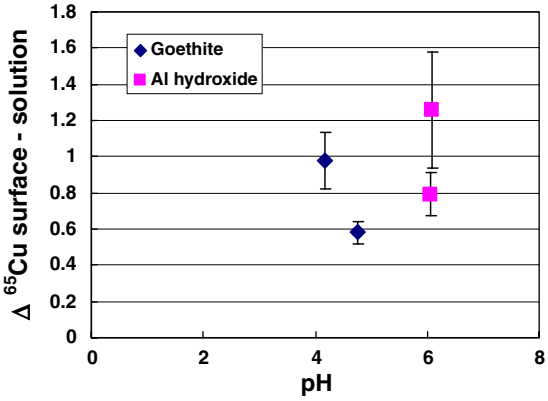


Fig. 10. Isotopic offset between solution and mineral surfaces (Eq. (3)) for copper adsorption on metal oxy(hydr)oxides as a function of pH. The error bars reflect the analytical uncertainty of MC-ICP-MS measurements; the experimental propagated errors due to uncertainty on $[Cu^{2+}]_{tot}$ analysis in solid and solution are smaller.

0.2‰ and 0.8 ± 0.2‰, respectively (Table 2, series 6). No systematic effect of pH or surface loading on the magnitude of isotopic fractionation could be established (Fig. 10).

## 4. DISCUSSION

### 4.1. Comparison with zinc isotope fractionation

The extent of Cu isotopic fractionation during the inorganic sorption processes is much higher than that following Zn sorption onto minerals such as goethite, birnessite, pyrolusite, corundum, and $Al(OH)_3$: $\Delta^{66}$Zn(solid-solution) = −0.20 ± 0.03, −0.17 ± 0.06, 0.10 ± 0.03, 0.10 ± 0.09, 0.13 ± 0.12‰, respectively (Pokrovsky et al., 2005b). At the same time, the isotopic shift induced by Zn sorption on ferrihydrite, hematite and amorhous ferric oxyhydroxide can achieve ±0.5–0.6‰ (Cacaly et al., 2004; Balistrieri et al., 2008). Icopini et al. (2004) studied Fe isotope fractionation upon sorption of $Fe^{2+}$(aq) to goethite under anaerobic conditions and reported $Fe(II)_{sorbed}$–$Fe(II)_{aq}$ fractionation of +2.1‰, which is similar both in sign and in magnitude to $Cu^{2+}$(aq) sorption onto goethite documented in the present work.

At the same time, Cu isotopic fractionation induced by the adsorption processes at the microorganism-solution interface in neutral solutions are of the same order of magnitude as those for Zn (i.e., 0.1–0.4‰). Indeed, irreversible incorporation of Zn in cultured marine and freshwater diatoms and adsorption on freshwater diatom cells produce an enrichment in heavy isotope compared to aqueous solution ($\Delta^{66}$Zn(solid-solution) = 0.1–0.2‰ (±0.05) and 0.3–0.4‰ (±0.1), respectively (Gélabert et al., 2006).

### 4.2. Thermodynamic stability of complexes

At the present time, the molecular mechanisms responsible for fractionation of stable isotopes of metals between solid and aqueous phases remain poorly understood. As a general rule (i.e., Lemarchand et al., 2005) and as follows from quantum mechanical considerations (Criss, 1999), the heavier isotope (i.e., $^{65}$Cu) should concentrate in the species in which it is most strongly bound (for example, tetrahedral adsorbed metal with shorter metal-O bonds compared to octahedral metal in solution). Among the tetrahedrally coordinated adsorbed species, it is the least stable complex that should be the most depleted in $^{65}$Cu. The first "macroscopic" test of this hypothesis was performed by comparing the average isotopic offset $\Delta^{65}$Cu(solid-solution) observed for oxy(hydr)oxides with the intrinsic surface stability constant for Eq. (6) measured in this study. Although gibbsite produces higher fractionation of Cu, its stability constant for Cu adsorption is lower, thus no simple correlation is observed. A similar conclusion has been reached for Zn adsorption on various metal oxides and hydroxides (Pokrovsky et al., 2005b). Secondly, we compared the Langmurian adsorption constant (Eq. (9)) for different bacterial species. Within the uncertainty of our measurements, no systematic variations of isotopic offset with the adsorption constant at neutral pH (4–6) can be detected. In contrast, a larger isotopic shift for Cu adsorption in acidic solutions on cells of rhizospheric soil bacteria *P. aureofaciens* after abundant EPS production (3rd series, experiment 2-1, 2-5 and 2-8 in Table 2), as compared to cells after poor EPS-synthesis (experiment 3-1, 3-5 and 3-9), is consistent with a somewhat higher $K_L$ (Eq. (9)) constant for the abundant EPS-producing culture (Table 1). However, this result has to be treated with caution as the pH range of isotopic measurements (1.8–3.3) and that of $K_L$ determination (5.8–6.1) is not the same. Therefore, in addition to thermodynamic stability of complexes, other

factors such as the structural parameters of adsorbed copper should be considered.

### 4.3. Structure of Cu complexes

Copper(II)–aqua complex $[Cu(H_2O)_6]^{2+}$ can be represented by a $CuO_6$ octahedron having axial distortion caused by the Jahn–Teller effect (Hathaway et al., 1987). This distorted octahedron has four equatorial Cu–O distances at $1.97 \pm 0.01$ Å and two axial oxygens at $2.24 \pm 0.03$ Å with 13.7% of disorder, according to an EXAFS study by Korshin et al. (1998). Another representation of distorted octahedron includes 2 Cu–O bonds of 1.97 Å, two of 2.00 Å and two axial bonds of 2.32 Å length (Farquhar et al., 1997). A quantum mechanical simulation suggests four equatorial oxygens at 2.0 Å and two axial O atoms at 2.14 Å (Korshin et al., 1998). A recent study based on neutron diffraction and first-principle molecular dynamics revealed that the solvated Cu complex undergoes frequent transformations (on the level of ps) between square pyramidal and trigonal bipyramidal configurations with $R_{Cu-O} = 1.96$ Å in the first solvation shell, with the sixth O atom situated in the 3.02–3.44 Å range (Pasquarello et al., 2001).

Adsorption of Cu(II) on at least some mineral surfaces brings about the formation of inner-sphere complexes with Cu–O distances that are shorter than those in aqueous solutions. For example, Cu(II) adsorbed on boehmite surfaces was reported to be coordinated by four oxygens in an axially symmetric ligand field with Cu–O bond distances of 1.93–1.94 Å (Weesner and Bleam, 1997). In the case of Cu adsorption onto goethite, Cu–O distances of 1.90 Å were reported (Lin et al., 2004). For Cu adsorbed on soil minerals (clays, quartz) and on goethite, the distances for four equatorial Cu–O bonds of 1.93–1.94 Å were reported (Parkman et al., 1999 and Boudesocque et al., 2007, respectively). A recent study by Peacock and Sherman (2004) revealed that Cu adsorbs onto goethite at pH 4.7–6.4 in the form of inner-sphere bidentate mononuclear complexes by corner-sharing with two or three edge-sharing $Fe(O,OH)_6$ polyhedra. The distances of the first coordination sphere reported in this work are, again, shorter than those in aqueous solutions: 1.92 Å for the first two Cu-$(OH)_2$ bonds. Copper adsorption onto kaolinite occurs via inner-sphere mononuclear complexes formed by corner-sharing with two or three edge-sharing $Al(O,OH)_6$ polyhedra (Peacock and Sherman, 2005). At pH 5.8 and 6.5, the copper first-shell coordination environment has 1 O at 1.85 Å, 2 O at 1.95-1.97 Å and 1 O at 2.05 Å. Assuming that kaolinite > AlOH sites can be considered an analog of gibbsite surface centers, the structure of adsorbed Cu complexes is more 'compact' with a smaller number of first shell neighbors. Therefore, a reduction of the Cu coordination number from 6 to 4–5 via formation of tetrahedral Cu–O–Fe to Cu–O–Al complexes with shorter Cu–O bonds than aqueous solution may produce an enrichment of $^{65}Cu$ on the oxide surface consistent with results of the present study ($\Delta^{65}Cu$(-solid-solution) = +0.6 to +1.3‰ (±0.15‰) as the heavier isotope should concentrate in the species to which it is bounded most strongly (i.e., Criss, 1999).

To our knowledge, there is no structural EXAFS information for Cu sorbed onto bacteria included in this work. Therefore, we will analyze existing literature data on the structure of Cu complexes with: (i) cell surface polysaccharides, and (ii) different organic substances including natural organic matter having functional groups similar to those of the bacteria. First we consider the case of Cu binding to organic substances at circumneutral pH range.

Carboxylate groups of the cell surface polysaccharides are expected to be deprotonated above pH 3.5 as measured $pK_a$ values of alginic acid and microbially produced exopolysaccharides are close to 3.4 (Lamelas et al., 2005, 2006), in agreement with values corresponding to the carboxylic groups of the mannuronic (3.38) and guluronic (3.65) acids (Haug, 1961). Carboxylate moieties of the cell surface have been demonstrated to be the primary sites of divalent metals binding to the biological surfaces in circumneutral pH range (Beveridge and Murray, 1980; Fein et al., 1997; Sarret et al., 1998; Tiemann et al., 2002; Pokrovsky et al., 2005a; Guiné et al., 2006). Nagy et al. (1998) studied Cu interaction with extracellular polysaccharide hyaluronate (glucosamino-glycan) and found distorted Cu–O octahedron with average distances (2.00 Å, equatorial and 2.48 Å, axial), which is not very different from the hexaaqua Cu(II) ion. Moreover, hyaluronate ligand is coordinated to the Cu(II) ion in a macrochelate manner, without formation of strong 5 or 6 membered chelate rings. The distances and coordinations reported for Cu complexes with a number of other polysaccharides and individual organic compounds, both in solid state and in aqueous solutions (cf., Nagy et al., 1998; Bosco et al., 2002), are quite similar to those of the $Cu(H_2O)_6^{2+}$ ion (Nagy and Szorcsik, 2002). Assuming that the cell surface polysaccharides of Gram-negative rhizospheric bacteria, anaerobic phototrophs, and external layers of cyanobacteria and diatoms studied in this work can be approximated by commercial polysaccharides, we can conclude that, at circumneutral pH, the first-neighbor structure of Cu complexes in the EPS of bacteria and in solution is very close and, thus, little fractionation can be expected.

The interaction of Cu(II) with organic surfaces revealed that, in neutral solutions, adsorbed Cu is present in the form of distorted octahedral, including square planar arrangement of 4 equatorial oxygen atoms at 1.94–1.96 Å and two axial oxygens at 2.31–2.34 Å (Fabaceous shrub, Sahi et al., 2007; lignocellulose, Dupont et al., 2002; wheat straw cell wall, Merdy et al., 2002). Binding of copper to humic acid at pH 4 produces an octahedron having four bonds at 1.93 Å and two bonds at 2.10 Å with 8.8% of disorder (Korshin et al., 1998), and the binding of Cu to humate at pH 4, 5 and 6 yields a tetragonally-distorted octahedra involving four oxygens of ligands (1.94 Å) and two oxygens of water at 2.00–2.02 Å at the first coordination shell and four C atoms at the second coordination shell as measured by EXAFS (Xia et al., 1997). The bond network analysis predicted that Cu(II) in humate would be surrounded by four oxygens from ligand at 2.04 Å and two oxygens from water at 2.19 Å (Xia et al., 1997). The absence of a second shell contribution in Cu-humic substances

or Cu-carboxylic resins was interpreted as a formation of outer-sphere complexes, that is, Cu adsorbed in a hydrated form $Cu(H_2O)_6^{2+}$ and/or a very distorted average geometry (Karlsson et al., 2006). Therefore, coordination of copper complexed with organic material at circumneutral pHs suggests a carboxylate-involved monodentate or bidentate environment, not very different from that in solution in terms of bond distances, coordination numbers and the level of dissymmetry. This type of binding most likely governs Cu interaction with external layers of bacterial biomass. Therefore, one should not expect any significant isotopic fractionation between aqueous solution and biological surfaces, in agreement with the results of the present study.

There is very little structural data available for Cu binding with organic substances in acidic solutions (pH 3.5). Parsons et al. (2002) reported that for Cu(II) bound to a hop plant (*Humulus lupulus*), Cu–O distances are longer at pH 2 as compared to pH 5. Since carboxylate functional groups play a critical role in the biosorption of Cu(II) by hop biomass (Hejazi, 2001), this indicates that the light isotope enrichment of organic surfaces is possible, which is consistent with the measurements of this study. Another line of evidence is found from available data on divalent metals interacting with Gram-positive bacteria, such as *Bacillus subtilis* (Kelly et al., 2002; Boyanov et al., 2003; Johnson et al., 2006). The outer membrane of the Gram-negative bacteria studied in this work contains phospholipids, lipoproteins, lipopolysaccharides, and proteins but, unlike Gram-positive bacteria, they do not include teichoic and teichuronic acid constituents (Beveridge, 1999). It has been suggested that the negatively charged phosphoryl groups in the core-lipid A region of the LPS (which are common to all four strains) are the most important sites involved in metal binding by *Pseudomonas aeruginosa* (Langley and Beveridge, 1999). Sokolov et al. (2001) proposed the presence of phosphodiester sites at low pH for Gram-negative bacteria. Since phospholipids have phosphoryl groups in the same local coordination environment as the phosphoryl groups in teichoic acid, recent data on Gram-positive bacteria can serve as a guide for understanding Cu interaction with Gram-negative bacteria.

Boyanov et al. (2003) showed that Cd adsorbed on *Bacillus subtilis* exhibited monodentate Cd-$PO_4$ complexes in acid solutions (pH < 4) and Cd-carboxylate bidentate complexes in neutral to alkaline solutions. For adsorbed metal, coordination number progressively decreases from $5.8 \pm 0.2$ at pH 3.4 to $4.8 \pm 0.2$ at pH ~6. Consistent with this finding, Kelly et al. (2002) argued that $UO_2^{2+}$ at low pH (1.67) binds to protonated phosphoryl group via monodentate complexes with 1 P atom at 3.64 Å. With increasing pH, $UO_2^{2+}$ increasingly binds to bacterial surface carboxyl functional groups (inner-sphere bidentate complex) with U–C distance of 2.89 Å. Molecular dynamics simulations suggest that, when coordinated with the phosphoryl group of teichoic acid, the Pb is preferentially bound in a monodentate structure with oxygen. Furthermore, for both Cd and Pb, the carboxylate ligands are more favored than those involving the phosphoryl groups of teichoic acid (Johnson et al., 2006).

Assuming these divalent metals can serve as analogs of $Cu^{2+}$, one can conclude that the adsorption of copper on bacteria in acidic solutions via monodentate phosphoryl complexes involves larger coordination numbers and longer bond distances. The bonds involved in these complexes are not as strong as those of the bidentate carboxylates. Therefore, one would expect an impoverishment of $^{65}Cu$ on the bacterial surface in acidic solutions consistent with results of quantum mechanical calculations, which predict that the heavier isotope should concentrate in the species in which it is bounded most strongly (Criss, 1999) (i.e., Cu hexaaqua complex or adsorbed carboxylate). This is consistent with negative isotopic offset measured in this study $\Delta^{65}Cu(\text{solid-solution}) = -0.6$ to $-1.8‰$ for soil *P. aureofaciens* at pH 1.8–3.3.

One should also consider that outer-sphere complexes of Cu, formed due to the presence of an overhelming negative charge (deprotonated carboxylate and phosphodiester functional groups), may partially control the isotopic fractionation. However, since the cell surface charge is dependent on pH and ionic strength and can differ between microbial species, the importance of outersphere complexes might change with pH, ionic strength, growth time and other parameters. At the present time, given the paucity of the data on how outer-sphere complexes control isotopic shift, as well as relevant structural information, further work is necessary to reveal the molecular mechanisms of fractionation involved in this kind of interaction.

## 5. CONCLUSIONS

The change of copper isotopic composition during its incorporation and adsorption onto viable bacteria and inorganic oxy(hydr)oxides, assessed in this work for the first time, reveals important constraints on biotic vs. abiotic fractionation mechanisms in surficial aquatic environments. The effect of various "external" parameters such as pH, exposure time, and copper and solid concentrations in solution on the fractionation factor were tested. It was found that only a pH decrease is capable of inducing significant isotopic shift ($0.6–1.8 \pm 0.05‰$) between solution and the bacterial surface. In the circumneutral pH range (4–7) both reversible short-term adsorption and assimilation during cell growth produced isotopic shifts comparable to the experimental uncertainty ($\pm 0.2‰$). Therefore, the interaction of aquatic photosynthetic microorganisms with Cu(II) in neutral well oxygenated solutions, such as surface waters, should not yield significant isotopic fractionation. In contrast, enrichment of heavy isotopes on the solid surface of Fe and Al oxy(hydr)oxides in solution produces an isotopic offset of $\Delta^{65}Cu(\text{solid-solution}) = 0.6–1.3‰$ ($\pm 0.1‰$). The last result corroborates the previous work of Mathur et al. (2005), who reported strong heavy Cu isotope enrichment on metal hydroxide precipitates on the external membranes of *Thiobaccilus ferrooxidans*, and the recent result of Balistrieri et al. (2008), who reported $\Delta^{65}Cu(\text{solid-solution}) = 0.73 \pm 0.08‰$ for Cu adsorption onto amorphous ferric oxyhydroxide.

The magnitude of Cu isotopic fractionation between bacterial or mineral surface and aqueous solution can not

be correlated with the value of the adsorption reaction stability constant and/or the surface sites densities. The potential effects of kinetic vs. equilibrium isotope effects during adsorption processes may explain measurable non-systematic variation of Cu-isotope fractionation factors in some experiments such as Cu sorption on metal oxy(hydr)oxides (series 6, Table 2) or short-term reversible adsorption on *Rhodobacter* sp. (series 4, Table 2). In addition, the effect of surface coverage on Cu-isotope fractionation can be also pronounced. Nevertheless, results on Cu isotopic fractionation are consistent with structural analysis of adsorbed and aqueous copper complexes based on existing EXAFS and ab initio modeling data. In accord with the general principles of isotope fractionation derived from quantum mechanical calculations, the heavier isotope ($^{65}$Cu) concentrates in the species in which it is bounded most strongly (i.e., oxide surface compared to aqueous solutions and bidentate carboxylates on the surface of microorganisms at neutral pHs compared to monodentate surface phosphoryl groups in acidic solutions). Indeed, the bond strengths of Cu complexes tend to decrease from oxides, to carboxylates, to phosphoryl groups, thereby supporting the observation that oxides are the most isotopically enriched, carboxylates are less isotopically enriched, and phosphoryl groups are the least isotopically enriched species.

Overall, the magnitude of copper isotopic fractionation during adsorption processes ($\Delta^{65}$Cu(solid-solution) = +1.3‰ to −1.8‰ (±0.1‰)) exceeds that of zinc by a factor of 5–10 and it is comparable with the fractionation of iron (Icopini et al. (2004)), molybdenum (Anbar, 2004; Barling and Anbar, 2004) and germanium (Galy et al., 2002). New measurements of the Cu isotopic composition in rivers, plankton and soils are necessary to compare these laboratory results with Cu geochemistry in natural settings and to further test the use of Cu isotopes for tracing surface processes.

## ACKNOWLEDGMENTS

We are grateful to C. Daughney, L. Wasylenki, L. Spadini, O. Rouxhel and an anonymous reviewer whose insight and thorough reviews greatly improved the manuscript. This work was supported by the French Ministry of International Affaires exchange program ECO-NET and by the Russian Foundation for Basic Research, Project No. 07-04-00651a. We thank A. Ciocarlan for invaluable help during bacterial culture process.

## REFERENCES

Allison J. D., Brown D. S. and Novo-Gradac K. J. (1991) MINTEQA2/PRODEFA2, *A Geochemical Assessment Model for Environmental Systems. Version 3.0 User's Manual*. U.S. EPA, Athens, GA, 106 pp.

Albarède F. (2004) The stable isotope geochemistry of copper and zinc. *Rev. Mineral. Geochem.* **55**, 409–427, Mineral. Soc. Am..

Alcacio T. E., Hesterberg D., Chou J. W., Martin J. D., Beauchemin S. and Sayers D. E. (2001) Molecular scale characteristics of Cu(II) bonding in goethite–humate complexes. *Geochim. Cosmochim. Acta* **65**, 1355–1366.

Anbar A. D. (2004) Molybdenum stable isotopes: observations, interpretations and directions. *Rev. Mineral. Geochem.* **55**, 429–454, Mineral. Soc. Am.

Anbar A., Roe J., Barling J. and Nealson K. (2000) Nonbiological fractionation of iron isotopes. *Science* **288**, 126–128.

Anbar A. D. and Rouxe l. O. (2007) Metal stable isotopes in paleoceanography. *Annu. Rev. Earth Planet. Sci.* **35**, 717–746.

Archer C. and Vance D. (2004) Mass discrimination correction in multiple-collector plasma source mass spectrometry: an example using Cu and Zn isotopes. *J. Anal. At. Spectrom.* **19**, 656–665.

Balistrieri L. S., Borrok D. M., Wanty R. B. and Ridley W. I. (2008) Fractionation of Cu and Zn isotopes during adsorption onto amorhous Fe(III) oxyhydroxide: Experimental mixing of acid rock drainage and ambient river water. *Geochim. Cosmochim. Acta* **72**, 311–328.

Barling J. and Anbar A. D. (2004) Molybdenum isotope fractionation during adsorption by manganese oxides. *Earth Planet. Sci. Lett.* **217**, 315–329.

Beard B., Johnson C., Skulan J., Nealson K., Cox L. and Sun H. (2003) Application of Fe isotopes to tracing the geochemical and biological cycling of Fe. *Chem. Geol.* **195**, 87–117.

Behrens U. and Ringpfeil M. (1963) Verfahren zur Herstellung von Fructose, insbesondere fur Infusionswecke. Pat. 24763. DDR. 1963. WP 30h/72537.

Bermin J., Vance D., Archer C. and Statham P. J. (2006) The determination of the isotopic composition of Cu and Zn in seawater. *Chem. Geol.* **226**, 280–297.

Beveridge T. J. and Murray R. (1980) Sites of metal deposition in the cell wall of *Bacillus subtilis*. *J. Bacteriol.* **141**, 876–887.

Beveridge T. J. (1999) Structures of Gram-negative cell walls and their derived membrane vesicles. *J. Bacteriol.* **181**, 4725–4733.

Borrok D., Fein J. B., Tischler M., O'Loughlin E., Meyer H., Liss M. and Kemner K. M. (2004) The effect of acidic solutions and growth conditions on the adsorptive properties of bacterial surfaces. *Chem. Geol.* **209**, 107–119.

Borrok D. M., Nimick D. A., Wanty R. B. and Ridley W. I. (2008) Isotopic variations of dissolved copper and zinc in stream waters affected by historical mining. *Geochim. Cosmochim. Acta* **72**, 329–344.

Bosco M., Miertus S., Turchini S., Prosperi T., Ascone I. and Rizzo R. (2002) Structural studies on polygalacturonate gels: an EXAFS investigation combined with molecular modeling. *Carbohyd. Polym.* **47**, 15–26.

Boudesocque S., Guillon E., Alpincourt M., Marceau E. and Stievano L. (2007) Sorption of Cu(II) onto vineyard soils: macroscopic and spectroscopic investigations. *J. Colloid Interf. Sci.* **307**, 40–49.

Boyanov M. I., Kelly S. D., Kemner K. M., Bunker B. A., Fein J. B. and Fowle D. A. (2003) Adsorption of cadmium to *Bacillus subtilis* bacterial cell walls: a pH-dependent X-ray absorption fine structure spectroscopy study. *Geochim. Cosmochim. Acta* **67**, 3299–3311.

Brantley S., Liermann L. and Bullen T. (2001) Fractionation of Fe isotopes by soil microbes and organic acids. *Geology* **29**, 535–538.

Cacaly S., Marechal C., Juillot F., Guyot F. and Benedetti M (2004) Zn isotopes fractionation upon sorption and precipitation. Abstracts of the 13th Annual V.M. Goldschmidt Conference, June 5–11, Copenhagen, Denmark. *Supplement to Geochim. Cosmochim. Acta*, 68/11S, p. A366.

Claessens J. and Van Cappellen P. (2007) Competitive binding of $Cu^2$ and $Zn^{2+}$ to live cells of Schewanella putrefaciens. *Environ. Sci. Technol.* **41**, 909–914.

Criss R. E. (1999) *Principles of Stable Isotope Distribution*. Oxford University Press, Oxford.

Davis T. A., Volesky B. and Mucci A. (2003) A review of the biochemistry of heavy metal biosorption by brown algae. *Water Res.* **37**, 4311–4330.

Daughney C. J., Fein J. B. and Yee N. (1998) A comparison of the thermodynamics of metal adsorption onto two common bacteria. *Chem. Geol.* **144**, 161–176.

Dittrich M. and Sibler S. (2005) Cell surface groups of two picocyanobacteria strains studied by zeta potential investigations, potentiometric titration, and infrared spectroscopy. *J. Colloid Interf. Sci.* **286**, 487–495.

Dupont L., Guillon E., Bouanda J., Dumonceau J. and Alpincourt M. (2002) EXAFS and XANES studies of retention of copper and lead by a lignocellulosic biomaterial. *Environ. Sci. Technol.* **36**, 5062–5066.

Ehrlich S., Butler I., Halicz L., Rickard D., Oldroyd A. and Matthews A. (2004) Experimental study of the copper isotope fractionation between aqueous Cu(II) and covellite, CuS. *Chem. Geol.* **209**, 259–269.

Emnova E., Tate III R. L., Gimenez D., Dascaliuc A., Toma S., Gojinetschi O. and Senicovscaia I. (2005) Reduction of metal and water stress of soybean by inoculation with exopolysccharide producing strains of *Pseudomonas* sp. In: *II International Symposium: Advanced Biological Technologies and their Impact on Economy* "*Natural products: Technologies for their Capitalization in Agriculture, Medicine, and Food Industry*", March 1–3, pp. 128–136.

Emnova E. E., Varbanets L. D., Vasiliev V. N., Ciocarlan A. G., Brovarskaia O. S., Caunova N. Ju., Ganea O. G. and Toma S. I. (2007) Properties of exopolysaccharides from rhizospheric fluorescent bacteria of *Pseudomonas genus*. *Bull. Moldovan Acad. Sci.-Life Sci.* **1**(310), 14–20.

Farquhar M. L., Vaughan D. J., Hughes C. R., Charnock J. M. and England K. E. R. (1997) Experimental studies of the interaction of aqueous metal cations with mineral substrates: lead, cadmium, and copper with perthitic feldspar, muscovite, and biotite. *Geochim. Cosmochim. Acta* **61**, 3051–3064.

Fein J. B., Daughney C. J., Yee N. and Davis T. A. (1997) A chemical equilibrium model for metal adsorption onto bacterial surfaces. *Geochim. Cosmochim. Acta* **61**, 3319–3328.

Fein J. B., Martin A. M. and Wightman P. G. (2001) Metal adsorption onto bacterial surfaces: development of a predictive approach. *Geochim. Cosmochim. Acta* **65**, 4267–4273.

Fowle D. A. and Fein J. B. (1999) Competitive adsorption of metal cations onto two Gram positive bacteria: testing the chemical equilibrium model. *Geochim. Cosmochim. Acta* **63**, 3059–3067.

Fowle D. A. and Fein J. B. (2000) Experimental measurements of the reversibility of metal–bacteria adsorption reactions. *Chem. Geol.* **168**, 27–36.

Galy A., Pokrovsky O. S. and Schott J. (2002) Ge-isotopic fractionation during its sorption on goethite: an experimental study. Abstracts of the VM Goldschmidt Conference, August 18–23, Davos, Switzerland, *Supplement to Geochim. Cosmochim. Acta*, *66*, p. A259.

Gélabert A., Pokrovsky O. S., Schott J., Boudou A., Feurtet-Mazel A., Mielczarski J., Mielczarski E., Mesmer-Dudons N. and Spalla O. (2004) Study of diatoms/aqueous solution interface. I. Acid–base equilibria, surface charge and spectroscopic observation of two freshwater peryphytic and two marine planctonic diatoms. *Geochim. Cosmochim. Acta* **68**, 4039–4058.

Gélabert A., Pokrovsky O. S., Viers J., Schott J., Boudou A. and Feurtet-Mazel A. (2006) Interaction between zinc and freshwater and marine diatom species: surface complexation and Zn isotope fractionation. *Geochim. Cosmochim. Acta* **70**, 839–857.

Gélabert A., Pokrovsky O. S., Schott J. and Boudou A. (2007) Cadmium and lead interaction with diatom surfaces: a combined thermodynamic and kinetic approach. *Geochim. Cosmochim. Acta* **71**, 3698–3716.

Gold C., Feurtet-Mazel A., Coste M. and Boudou A. (2003) Effect of cadmium stress on periphytic diatom communities in indoor artificial streams. *Freshwater Biol.* **48**, 316–328.

Gonzalez-Davila M. (1995) The role of phytoplankton cell on the control of heavy metal concentrations in seawater. *Marine Chem.* **48**, 215–236.

Gonzales-Davila M., Santana-Casiano J. M., Perez-Pena J. and Millero F. J. (1995) Binding of Cu(II) to the surface and excudates of the alga *Dunaliela tertiolecta* in seawater. *Environ. Sci. Technol.* **29**, 289–301.

Gonzalez-Davila M., Santana-Casiano J. M. and Laglera L. M. (2000) Copper adsorption in diatom cultures. *Marine Chem.* **70**, 161–170.

Guiné V., Spadini L., Muris M., Sarret G., Delolme C., Gaudet J.-P. and Martins J. M. F. (2006) Zinc sorption to cell wall components of three Gram-negative bacteria: a combined titration, modeling and EXAFS study. *Environ. Sci. Technol.* **40**, 1806–1813.

Hathaway B. J. (1987). In *Comprehensive Coordiantion Chemistry—The Synthesis Reactions Properties and Applications of Coordination Compounds*, vol. 5 (ed. G. Wilkinson et al.). Pergamon Press, pp. 533–774.

Haug A. (1961) Dissociation of alginic acid. *Acta Chem. Scand.* **15**, 950–952.

He L. M. and Tebo B. M. (1998) Surface charge properties of and Cu(II) adsorption by spores of the marine Bacillus sp, Strain SG-1. *Appl. Environ. Microbiol.* **64**, 1123–1129.

Hejazi M. (2001) *New Technology to Remove Toxic Metal Ions Using Hop Biomass: Use of Chemical Modification and X-ray Absorption Spectroscopy to Determine the Mechanism(s) of Metal Removal*. Ph.D. Thesis, University of Texas at El Paso, pp. 126

Hoffmann S. R., Shafer M. M. and Armstrong D. E. (2007) Strong colloidal and dissolved organic ligands binding copper and zinc in rivers. *Environ. Sci. Technol.* **41**, 6996–7002.

Icopini G. A., Anbar A. D., Ruebush S. S., Tien M. and Brantley S. L. (2004) Iron isotope fractionation during microbial reduction of iron: the importance of adsorption. *Geology* **32**, 205–208.

Johnson C. M., Beard B. L., Roden E. E., Newman D. K. and Nealson K. H. (2004) Isotopic constraints on biogeochemical cycling of Fe. *Rev. Mineral. Geochem.* **55**, 359–408, Mineral. Soc. Amer.

Johnson K. J., Cygan R. T. and Fein J. B. (2006) Molecular simulation of metal adsorption to bacterial surfaces. *Geochim. Cosmochim. Acta* **70**, 5075–5088.

Karlsson T., Persson P. and Skyllberg U. (2006) Complexation of copper(II) in organic soils and in dissolved organic matter—EXAFS evidence for chelate ring structures. *Environ. Sci. Technol.* **40**, 2623–2628.

Kelly S. D., Kemner K. M., Fein J. B., Fowle D. A., Boyanov M. I., Bunker B. A. and Yee N. (2002) X-ray absorption fine structure determination of pH-dependent U-bacterial cell wall interactions. *Geochim. Cosmochim. Acta* **66**, 3855–3871.

Klimmek S., Stan H.-J., Wilke A., Bunke G. and Buchholz R. (2001) Comparative analysis of the biosorption of cadmium, lead, nickel, and zinc by algae. *Environ. Sci. Technol.* **35**, 4283–4288.

Knauer K., Behra R. and Sigg L. (1997) Effects of free $Cu^{2+}$ and $Zn^{2+}$ ions on growth and metal accumulation in freshwater algae. *Environ. Toxicol. Chem.* **16**, 220–229.

Knauer K., Ahner B., Xue H. B. and Sigg L. (1998) Metal and phytochelatin content in phytoplankton from freshwater lakes

with different metal concentrations. *Environ. Toxicol. Chem.* **17**, 2444–2452.

Korshin G. V., Frenkel A. I. and Stern E. A. (1998) EXAFS study of the inner shell structure in copper(II) complexes with humic substances. *Environ. Sci. Technol.* **32**, 2699–2705.

Kunito T., Saeki K., Nagaoka K., Oyaizu H. and Matsumoto S. (2001) Characterization of copper-resistant bacterial community in rhizosphere of highly copper-contaminated soil. *Eur. J. Soil Biol.* **37**, 95–102.

Lamelas C., Avaltroni F., Benedetti M., Wilkinson K. J. and Slaveykova V. I. (2005). *Biomacromolecules* **6**, 2756–2764.

Lamelas C., Benedetti M., Wilkinson K. J. and Slaveykova V. I. (2006) Characterization of $H^+$ and $Cd^{2+}$ binding properties of the bacterial exopolysaccharides. *Chemosphere* **65**, 1362–1370.

Langley S. and Beveridge T. J. (1999) Effect of O-side-chain-lipopolysaccharide chemistry on metal binding. *Appl. Environ. Microbiol.* **65**, 489–498.

Larson P. B., Maher K., Ramos F. C., Chang Z., Gaspar M. and Meinert L. D. (2003) Copper isotope ratios in magmatic and hydrothermal ore-forming environments. *Chem. Geol.* **201**, 337–350.

Lemarchand E., Schott J. and Gaillardet J. (2005) Boron isotopic fractionation related to boron sorption on humic acid and the structure of surface complexes formed. *Geochim. Cosmochim. Acta* **69**, 3519–3533.

Lin S.-H., Kao H.-C., Cheng C.-H. and Juang R.-S. (2004) An EXAFS study of the structures of copper and phosphate sorbed onto goethite. *Colloids Surf. A: Physicochem. Eng. Aspects* **234**, 71–75.

Lützenkirchen J. (1999) The constant capacitance model and variable ionic strength: an evaluation of possible applications and applicability. *J. Coll. Interf. Sci.* **217**, 8–18.

Mathur R., Ruiz J., Titley S., Liermann L., Buss H. and Brantley S. (2005) Cu isotopic fractionation in the supergene environment with and without bacteria. *Geochim. Cosmochim. Acta* **69**, 5233–5246.

Maréchal C. N. (1998) *Géochimie des isotopes du cuivre et du zinc: méthode, variabilité naturelle et application océanographique*. Ph.D. Thesis, Ecole Normale Supérieure de Lyon, Université Claude Bernard—Lyon I, 261 pp.

Maréchal C. N. and Albarède F. (2002) Ion-exchange fractionation of copper and zinc isotopes. *Geochim. Cosmochim. Acta* **66**, 1499–1509.

Maréchal C. N., Telouk P. and Albarède F. (1999) Precise analysis of copper and zinc isotopic compositions by plasma-source mass spectrometry. *Chem. Geol.* **156**, 251–273.

Maréchal C. N. and Sheppard S. M. F. (2002) Isotopic fractionation of Cu and Zn between chloride and nitrate solutions and malachite or smithsonite at 30° and 50 °C. Goldschmist 2002 Conference, Davos. *Geochim. Cosmochim. Acta* **66**(15A), A484.

Markl G., Lahaye Y. and Schwinn G. (2006) Copper isotopes as monitors of redox processes in hydrothermal mineralization. *Geochim. Cosmochim. Acta* **70**, 4215–4228.

Martell A. E., Smith R. M. and Motekaitis R. J. (1997) *NIST Critically Selected Stability Constants of Metal Complexes. Database software Version 3.0*. Texas A & M University, College Station, TX.

Merdy P., Guillon E., Dumonceau J. and Alpincourt M. (2002) Spectroscopic atusy of copper(II)–wheat straw cell wall residue surface complexes. *Environ. Sci. Technol.* **36**, 1728–1733.

Meyer J. M. and Abdallah M. A. (1978) The fluorescent pigment of *Pseudomonas fluorescens* biosynthesis, purification and physicochemical properties. *J. Gen. Microb.* **107**, 319–328.

Mirimanoff N. and Wilkinson K. J. (2000) Regulation of Zn accumulation by a freshwater Gram-positive bacterium (*Rhodococcus opacus*). *Environ. Sci. Technol.* **34**, 616–622.

Nagy L., Yamashita S., Yamaguchi T., Sipos P., Wakita H. and Nomura M. (1998) The local structures of Cu(II) and Zn(II) complexes on hyaluronate. *J. Inorg. Biochem.* **72**, 49–55.

Nagy L. and Szorcsik A. (2002) Equilibrium and structural studies on metal complexes of carbohydrates and their derivatives. *J. Inorg. Biochem.* **89**, 1–12.

Ngwenya B. T., Suthermand I. W. and Kennedy L. (2003) Comparison of the acid–base behaviour and metal adsorption characteristics of a Gram-negative bacterium with other strains. *Appl. Geochem.* **18**, 527–538.

Parkman R. H., Charnock J. M., Bryan N. D., Livens F. R. and Vaughan D. J. (1999) Reactions of copper and cadmium ions in aqueous solution with goethite, lepidocrocite, mackinawite, and pyrite. *Am. Mineral.* **84**, 407–419.

Parsons J. G., Hejazi M., Tiemann K. J., Henning J. and Gardea-Torresdey J. L. (2002) An XAS study of the binding of copper(II), zinc(II), chromium(III) and chromium(VI) to hop biomass. *Microchem. J.* **71**, 211–219.

Pasquarello A., Petri I., Salmon P. S., Parisel O., Car R., Tóth E., Powell D. H., Fischer H. E., Helm L. and Merbach A. E. (2001) First salvation shell of the Cu(II) aqua ion: evidence for fivefold coordination. *Science* **291**, 856–859.

Peacock C. L. and Sherman D. M. (2004) Copper(II) sorption onto goethite, hematite and lepidocrocite: a surface complexation model based on ab initio molecular geometries and EXAFS spectroscopy. *Geochim. Cosmochim. Acta* **68**, 2623–2637.

Peacock C. L. and Sherman D. M. (2005) Surface complexation model for multisite adsorption of copper(II) onto kaolinite. *Geochim. Cosmochim. Acta* **69**, 3733–3745.

Pfennig N. and Trüper H. G. (1989) Anoxygenic Phototrophic bacteria. In: *Bergey's Manual of Systematic Bacteriology*, vol. 3. Williams & Wilkins, Baltimore, USA, pp. 1635–1709.

Pichat S., Douchet C. and Albaréde F. (2003) Zinc isotope variations in deep-sea carbonates from the eastern equatorial Pacific over the last 175 ka. *Earth Sci. Planet Lett.* **210**, 167–178.

Pokrovsky O. S., Pokrovski G. S., Gélabert A., Schott J. and Boudou A. (2005a) Speciation of Zn associated with diatoms using X-ray absorption spectroscopy. *Environ. Sci. Technol.* **39**, 4490–4498.

Pokrovsky O. S., Viers J. and Freydier R. (2005b) Zinc stable isotope fractionation during its adsorption on oxides and hydroxides. *J. Colloid Interf. Sci.* **291**, 192–200.

Pokrovsky O. S., Pokrovski G. S., Schott J. and Galy A. (2006) Germanium adsorption on goethite and Ge coprecipitation with iron hydroxide: X-ray Absorption Spectroscopy (XAS) study and macroscopic characterization. *Geochim. Cosmochim. Acta* **70**, 3325–3341.

Rousset D., Henderson G. M. and Shaw S. (2004) Cu and Zn isotope fractionation during sorption experiments. *Geochim. Cosmochim. Acta* **68**(11), A36, Suppl. S..

Rouxel, O. D. (2002) Géochimie isotopique des métaux (Fe, Cu, Pb) et des metalloides (S, Se) dans la croûte océanique. Thesis Inst. Nat. Polytechnic Lorraine, Nancy.

Rouxel O., Fouquet Y. and Ludden J. N. (2004) Copper isotope systematics of the Lucky Strike, Rainbow, and Logatchev sea-floor hydrothermal fields on the Mid-Atlantic Ridge. *Econ. Geol.* **99**, 585–600.

Sahi S. V., Israr M., Srivastava A. K., Gardea-Torresdey J. L. and Parsons J. G. (2007) Accumulation, speciation and cellular localization of copper in *Sesbania drummondii*. *Chemosphere* **67**, 2257–2266.

Sarret G., Manceau A., Spadini L., roux J. C., Hazemann J.-L., Soldo Y., Eybert-Bérard L. and Menthonnex J. J. (1998) EXAFS determination of Pb, Zn complexing sites of *Penicillum chrysogenum* cell walls. *Environ. Sci. Technol.* **32**, 1648–1655.

Slaveykova V. I. and Wilkinson K. J. (2002) Physicochemical aspects of lead bioaccumulation by *Chlorella vulgaris*. *Environ. Sci. Technol.* **36**, 969–975.

Smiejan A., Wilkinson K. J. and Rossier C. (2003) Cd bioaccumulation by a freshwater bacterium, *Rhodospirillum rubrum*. *Environ. Sci. Technol.* **37**, 701–706.

Sokolov I., Smith D. S., Hederson G. S., Gorby A. and Ferris F. G. (2001) Cell surface electrochemical heterogeneity of the Fe(III)-reducing bacteria *Shewanella putrefaciens*. *Environ. Sci. Technol.* **35**, 341–347.

Soldo D. and Behra R. (2000) Long-term effects of copper on the structure of freshwater periphyton communities and their tolerance to copper, zinc, nickel and silver. *Aquatic Toxicol.* **47**, 181–189.

Stumm W. (1992) *Chemistry of the Solid–Water Interface*. John Wiley and Sons.

Sutherland I. W. (1982) Biosynthesis of microbial polysaccharides. *Adv. Microbiol. Physiol.* **23**, 79–150.

Sverjensky D. and Sahai N. (1996) Theoretical prediction of single-site surface-protonation equilibrium constants for oxides and silicates in water. *Geochim. Cosmochim. Acta* **60**, 3773–3797.

Tiemann K. J., Rascon A. E., Gamez G., Parsons J. G., Baig T., Cano-Aguilera I. and Gardea-Torresdey J. L. (2002) Heavy metal binding by inactivated tissues of *Solanum elaeagnifolium*: chemical and subsequent XAS studies. *Microchem. J.* **71**, 133–141.

Viers J., Oliva P., Nonell A., Gélabert A., Sonke J. E., Freydier R., Gainville R. and Dupré B. (2007) Evidence of Zn isotopic fractionation in a soil-plant system of a pristine tropical watershed (Nsimi, Cameroon). *Chem. Geol.* **239**, 124–137.

Weesner F. J. and Bleam W. F. (1997) X-ray absorption and EPR spectroscopic characterization of adsorbed copper(II) complexes at the boehmite (AlOOH) surface. *J. Colloid Interf. Sci.* **196**, 79–86.

Wu F. and Tanoue E. (2001) Isolation and partial characterization of dissolved copper-complexing ligands in streamwaters. *Environ. Sci. Technol.* **35**, 3646–3652.

Xia K., Bleam W. and Helmke P. A. (1997) Studies of the nature of Cu2+ and Pb2+ binding sites in soil humic substances using X-ray absorption spectroscopy. *Geochim. Cosmochim. Acta* **61**, 2211–2221.

Xue H. B., Stumm W. and Sigg L. (1988) The binding of heavy metals to algal surfaces. *Water Res.* **22**, 917–926.

Xue H. B. and Sigg L. (1990) Binding of Cu(II) to algae in a metal buffer. *Water Res.* **24**, 1129–1136.

Zhu X. K., O'Nions R. K., Guo Y., Belshaw N. S. and Rickard D. (2000) Determination of natural Cu-isotope variation by plasma-source mass spectrometry: implications for use as geochemical tracers. *Chem. Geol.* **163**, 139–149.

Zhu X. K., Guo Y., Williams R. J. P., O'Nions R. K., Matthews A., Belshaw N., Canters G. W., de Waal E. C., Weser U., Burgess B. K. and Salvato B. (2002) Mass fractionation of the transition metal isotopes. *Earth Planet Sci. Lett.* **200**, 47–62.

*Associate editor:* Christopher John Daughney